



**UNSW Renewable Hydrogen for Export Research and Development Project**  
**Photovoltaic Electrolysis towards Green Hydrogen Generation**  
**2018/RND014**



**End of Activity Report**

This activity received funding from ARENA as part of ARENA's Research and Development Program – Renewable Hydrogen Export

**Authors:** A/Prof Xunyu Lu, Scientia Prof Rose Amal, Dr Qingran Zhang, Dr Mark Keevers, Mr John Lasich, Prof Yansong Shen, Prof Chuan Zhao, Dr Rahman Daiyan

**Key Contributors:** Dr Jian Pan, Dr Yufei Zhao, Mr Yihao Shan, Mr David Cox, Dr Ivan Perez-Wurfl, Ms Xiaoying Wong, Prof Martin Green

Submitted January 2023

*Disclaimer: Please note that the views expressed herein are not necessarily the views of the Australian Government and the Australian Government does not accept responsibility for any information or advice contained here.*

## Table of Contents

Executive Summary .....	3
Abbreviations and Acronyms .....	5
1. Introduction .....	6
1.1 Context .....	6
1.2 Objectives .....	6
2. Outcomes .....	7
2.1 Overview .....	7
2.2 CPV receiver .....	9
2.3 Water electrolysis system .....	10
2.3.1 Design of efficient electrocatalysts .....	10
2.3.2 The effects of temperature and KOH concentration .....	12
2.3.3 The performance of customised water electrolyzers .....	13
2.4 Heat exchange systems .....	14
2.5 Integrated PVE systems .....	15
2.6 CFD modelling .....	23
2.7 Techno-economic analysis .....	25
3. Challenges Encountered and Lessons Learned .....	32
3.1 Water electrolyser cell .....	32
3.2 Accurate control and monitoring of temperature .....	32
3.3 Electrical integration between CPV and AWE .....	33
4. Commercialisation Prospects .....	33
5. Knowledge Sharing Activities .....	34
5.1. Events/Activities/Outreach .....	34
5.2 Publications .....	36
6. Conclusion and Future Plans .....	37
6.1 Conclusion .....	37
6.2 Future Plans .....	38
Reference .....	38

## Executive Summary

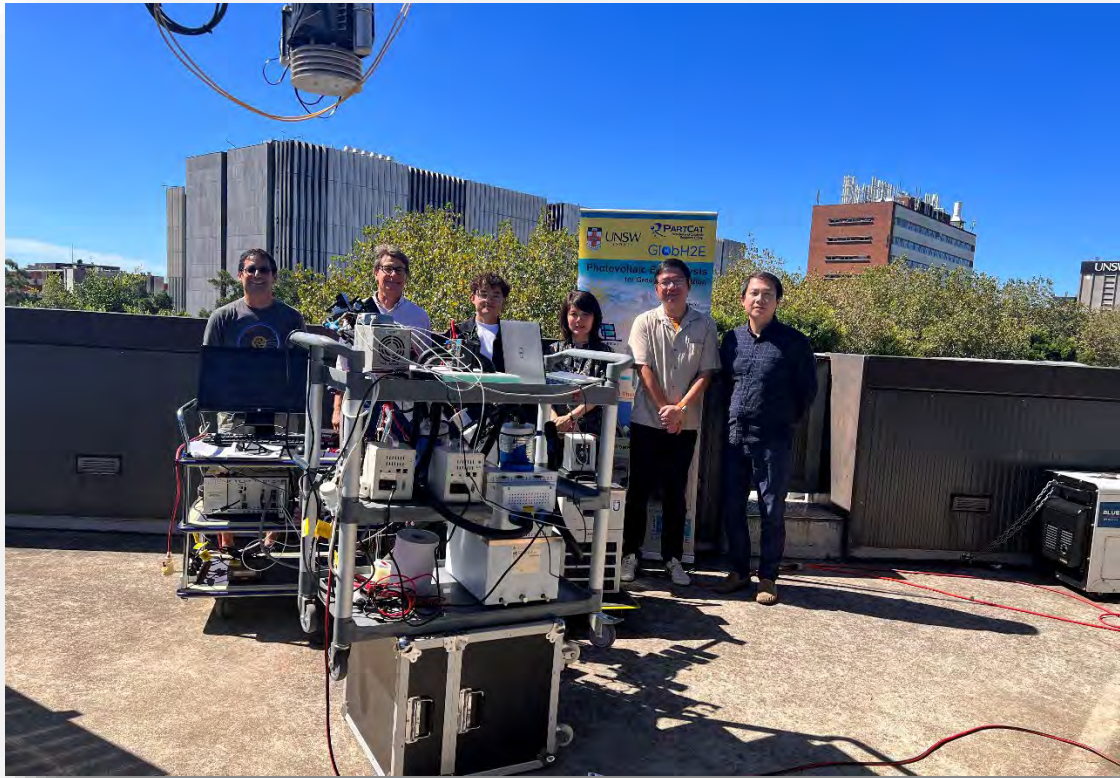
This document corresponds to the “End of Activity” report for the University of New South Wales Photovoltaic Electrolysis Research and Development Project: Photovoltaic Electrolysis to Generate Hydrogen. The project aimed to use photovoltaic electrolysis coupled with thermal energy obtained from concentrated photovoltaic devices to effectively improve the solar-to-hydrogen conversion efficiency.

The key thesis was to develop high-performance electrocatalysts that can catalyse the water electrolysis process efficiently. Moreover, the waste thermal energy generated by the concentrated photovoltaic (CPV) cells can also be harvested to heat the electrolyte to improve the sluggish water splitting kinetics. By using thermal and electrical energy obtained from sunlight, two state-of-the-art integrated photovoltaic-electrolysis (PVE) systems are established, showing a record-breaking solar-to-hydrogen (STH) conversion efficiency around 30% (excluding the lead losses) in a prototype 20 W system. The exceptional STH efficiency could lower the levelised cost of hydrogen produced via electrolysis to a great extent, thereby facilitating the large-scale implementation of this promising technology. Notably, the established PVE system is comprised of three main components: (i) a CPV module that produces both heat and renewable electricity; (ii) a customised alkaline water electrolyser that is electrically connected with the CPV module (via a custom built DC-DC ‘buck’ converter); and (iii) a custom-designed heat exchange system thermally connected with the cooling water loop in CPV module to transfer the heat from CPV device to water electrolysis system. In this project, two PVE systems with different capacities were developed and studied. First, to demonstrate the feasibility of harvesting both heat and electricity from a CPV module, a 1 kW PVE system was set up based on commercially available components. Then, to achieve the record-breaking STH efficiency, a 20 W PVE system was developed based on the customised alkaline water electrolyser and a CPV cell receiver. In addition to the two PVE systems, this project also includes (i) modelling the two-phase flow behaviour in flow channels; and (ii) conducting techno-economic feasibility studies.

**Achievement of Milestones:** The project has achieved all the aims, including all the milestones and deliverables (as planned and within budget), that this project set out to accomplish. It has successfully demonstrated the concept on which it was based, namely, that more affordable green H<sub>2</sub> could be produced from the high-performance PVE system enabled by the development of active electrocatalysts and effective device management.

**Outputs/Impacts:** The project has resulted in the successful development of an efficient and cost-effective water splitting electrocatalysis system, which has been integrated with a highly efficient Concentrate PV cell and receiver, as well as a top-performing DC-DC converter. This groundbreaking system has achieved a record-breaking STH efficiency of around 30%. The

computational modelling and techno-economic analysis within the scope of this project also allow for the detailed analysis of commercial potential of this emerging technology, providing a promising way to achieve cheaper green H<sub>2</sub> generation at practical rate. Thus far, the project work has led to 9 journal publications.



*Key researchers at UNSW (Left to right: Dr Ivan Perez-Wurfl, Dr Mark Keever, Mr Yihao Shan, Scientia Prof. Rose Amal, A/Prof Xunyu Lu and Dr Jian Pan).*

## Abbreviations and Acronyms

<b>3D</b>	3 Dimensional
<b>AEM</b>	Anion-Exchange-Membrane
<b>ARENA</b>	Australian Renewable Energy Agency
<b>AWE</b>	Alkaline Water Electrolyser
<b>Buck Eff</b>	Buck Efficiency
<b>CFD</b>	Computational Fluid Dynamic
<b>CI</b>	Chief Investigator
<b>CO<sub>2</sub></b>	Carbon dioxide
<b>CPV</b>	Concentrated Photovoltaic
<b>CST</b>	Concentrated Solar Thermal System
<b>DC</b>	Direct Current
<b>EC</b>	Electrolyser Cell
<b>EC Eff</b>	Electrolyser Cell Efficiency
<b>Eff</b>	Efficiency
<b>GW</b>	Giga Watt
<b>HAADF-STEM</b>	High-angle annular dark-field scanning transmission electron microscopy
<b>HER</b>	Hydrogen Evolution Reaction
<b>HX</b>	Heat Exchanger
<b>HySupply</b>	German-Australian Feasibility Study of Hydrogen
<b>J<sub>EC</sub></b>	Electrolyser Current Density
<b>LC<sub>H<sub>2</sub></sub> / LCOH</b>	Levelised Cost of Hydrogen
<b>MO</b>	Metal Oxides
<b>MPPT</b>	Maximum Power Point
<b>MW</b>	Mega Watt
<b>nm</b>	Nano metre
<b>NSW</b>	New South Wales
<b>O&amp;M</b>	Operation and Maintenance
<b>OER</b>	Oxygen Evolution Reaction
<b>PEM</b>	Proton-Exchange-Membrane
<b>PV</b>	Photovoltaic
<b>PVE</b>	Photovoltaic-Electrolysis
<b>PWM</b>	Pulse width modulation
<b>RHE</b>	Reversible Hydrogen Electrode
<b>RTD</b>	Resistance Temperature Detector
<b>SCE</b>	Saturated Calomel Electrode
<b>STE</b>	Solar-to-electricity
<b>STH</b>	Solar-to-hydrogen
<b>TRL</b>	Technology Readiness Level
<b>VOF</b>	Volume of Fluid

## **1. Introduction**

### *1.1 Context*

Australia has abundant solar power, thereby the development of efficient solar energy conversion and storage approaches would enable Australia to play a critical role in providing clean energy to society. Benefited from the significant technical advances in photovoltaic (PV) technology, the cost of PV cells has been reduced drastically during the past decade, which in turn spurs the prosperous development of techniques that can store the solar electricity either in its original form or in the chemical form (such as hydrogen). The photovoltaic-electrolysis (PVE) system, where the water electrolyzers are powered by PV cells, provides a promising way to store the excessive solar electricity in the form of hydrogen.[1] Apart from this, the hydrogen produced via PVE system is considered as green (with zero carbon footprint), while the traditional ways to produce hydrogen (such as natural gas reforming) inevitably emit large amounts of carbon dioxide. Nevertheless, the commercialisation of PVE systems is severely constrained by the high cost of hydrogen produced. The high cost of hydrogen from PVE systems stem from two factors: (i) low energy efficiency of the water electrolyzers caused by the lack of active and cost-effective catalyst materials and (ii) low STH efficiency of PVE systems originated from the mismatch between PV and electrolyzers as well as the poor system management that limits the effective use of solar energy. In this regard, there is an urgent call for the development of customised water electrolyzers with high energy efficiency and low cost, as well as integrated PVE systems with well-aligned components that can achieve record-breaking STH efficiencies.

### *1.2 Objectives*

The activity of this project aims to develop a PVE system capable of producing green H<sub>2</sub> with the STH efficiency around 30%, which can effectively lower the levelized cost of H<sub>2</sub> to pave its pathway for commercialisation in near future. The integrated PVE system comprises a CPV module with over 39% solar-to-electricity (STE) conversion efficiency, a customised high-performance DC-DC converter, a self-designed and manufactured heat exchanger and a high-performance alkaline water electrolyser assembled with cost-effective materials. Final deliverables for the Activity were to:

- 1) Develop suitable electrocatalysts that can enable the water electrolysis process to occur under large current densities with low overpotentials, including hydrogen evolution reaction (HER) catalysts and oxygen evolution reaction (OER) catalysts;
- 2) Optimise the water electrolysis performance in both single-cell and stack electrolyzers with the as-developed electrocatalysts towards hydrogen production of high energy efficiencies;
- 3) Design the prototype of a heat exchange system that can effectively harvest the thermal energy generated by CPV modules to heat the electrolyte in water electrolyzers;



- 4) Combine the customised water electrolysers with the CPV minimodule to form a 20 W integrated PVE system with the record-breaking STH efficiency up to 30% under concentrated sunlight irradiation;
- 5) Scale-up the designs in 20 W PVE setup to a 1 kW system using commercially available components that can be both thermally and electrically integrated with CPV module from RayGen;
- 6) Establish a computational model which can predict and describe the possible limitations in electrolyser components so that guidance can be given to system scale-up;
- 7) Conduct techno-economic analysis to study the commercial feasibility of PVE technology in the Activity;

The End of Activity Report discloses key outcomes from the Activity and provides details on lessons learned, commercialisation prospects, knowledge-sharing undertakings and future research plan for PVE technology.

## 2. Outcomes

### 2.1 Overview



**Figure 1.** The integrated 1 kW PVE system. (Dr. Jian Pan was operating the alkaline water electrolyser stacks in the images)

Two PVE systems with different capacities are developed in this project. Firstly, to demonstrate the feasibility of harvesting both electricity and heat from the CPV modules for the performance enhancement of a water electrolyser, a 1 kW PVE setup was fabricated. This system is comprised of a commercial alkaline water electrolyser (model: LBE-C, Lightbridge), a customised high-performance DC-DC converter, a self-designed and manufactured heat exchanger, and Raygen's CPV module. The photo of the 1 kW integrated PVE system is shown in Figure 1. In this setup, the electrolyser is thermally and electrically coupled with the CPV module through the DC-DC converter and the customized heat exchanger. The heat exchanger harvests the heat from the hot water in the CPV cooling loop to raise







**Figure 2b.** Photo of the 20 W PVE system for producing green hydrogen with *STH* efficiencies up to 30%.

Details on the development and performance of each sub-system and the overall system can be found in the following sections.

## 2.2 CPV receiver

The 1 kW PVE system utilises a commercial RayGen module, including proprietary dense array of CPV cells and high performance heatsink. The 20 W PVE system uses a high efficiency CPV receiver consisting of a packaged commercial CPV cell (Azur Space 3C44) with efficiency exceeding 38%, a water cooled heatsink to control the CPV cell operating temperature (to 25°C in this experiment), an 8-inch diameter parabolic concentrating mirror with very high reflectance (99.7%) over the response range of the CPV cell (400-1800 nm), and a custom made iris aperture (using 3D printed plastic parts) to control the sunlight concentration up to 500 suns. The single CPV cell receiver emulates RayGen's commercial system in that it uses similar CPV cell and a mirror to concentrate the sunlight, albeit with a focus on highest efficiency.

## 2.3 Water electrolysis system

### 2.3.1 Design of efficient electrocatalysts

To endow the overall water electrolysis with a high performance, the design and development of efficient electrocatalysts that can exhibit a high activity (reflected by current density) under low overpotentials, robust stability and low cost are highly sought after. Thus, in this activity, several types of high-performance HER and OER electrocatalysts were developed with primarily cost-effective materials. Firstly, efficient OER electrocatalysts composed of transition metals were designed and fabricated to accelerate the sluggish water oxidation process that has been long hampering the water electrolysis performance. It is worth noting that the improvement of OER performance is normally limited by the scaling relationship of binding energy between different reaction intermediates (such as  $\text{OH}^*$  and  $\text{OOH}^*$ ) and the active sites, thereby leading to low OER performance that requires tremendous amounts of overpotential to deliver an acceptable current density (e.g.  $100 \text{ mA cm}^{-2}$ ). To this end, we have designed a novel composite catalyst that is comprised of multi-phase metal oxides (MO) to break the scaling relationship for OER performance enhancement. The catalyst is composed of nickel oxide and iron oxide, as shown in Figure 3. The two components contact intimately within the composite, forming numerous boundaries that are active to catalyse the OER. Moreover, to directly employ the as-fabricated OER electrocatalysts in the electrolyser without sacrificing the electrode conductivity and to improve the bubble dissipation efficiency, a free-standing electrode was constructed by growing the OER catalysts directly onto the Fe foam substrate via a facile method (Figure 3c). In this project, electrodes with varied surface area have been prepared ( $1 \text{ cm}^2$ ,  $4 \text{ cm}^2$ ,  $9 \text{ cm}^2$  and  $25 \text{ cm}^2$ ) for different application purposes. As a result, the as-fabricated OER electrodes exhibit superior catalytic performances towards the OER in alkaline media. As shown in Figure 4a, the electrode is capable of catalysing the OER at an onset potential as low as  $1.41 \text{ V}$  (vs. Reversible Hydrogen Electrode), corresponding to an overpotential of merely  $180 \text{ mV}$ . Moreover, at an overpotential of  $300 \text{ mV}$ , the electrode can deliver a high OER current density of  $1 \text{ A cm}^{-2}$ . These performances surpass the NiFe benchmark and other state-of-the-art catalysts (including those based on noble metals, such as  $\text{IrO}_x$  and  $\text{RuO}_2$ ) reported previously. The obtained free-standing electrode also exhibits prominent stability during OER in alkaline media (Figure 4b), showing negligible activity decay for nearly  $100 \text{ h}$  at the current density of  $100 \text{ mA cm}^{-2}$ . As such, the MO electrodes developed here were subsequently employed in the  $20 \text{ W}$  water electrolyser that is used for the prototype modular PVE system.

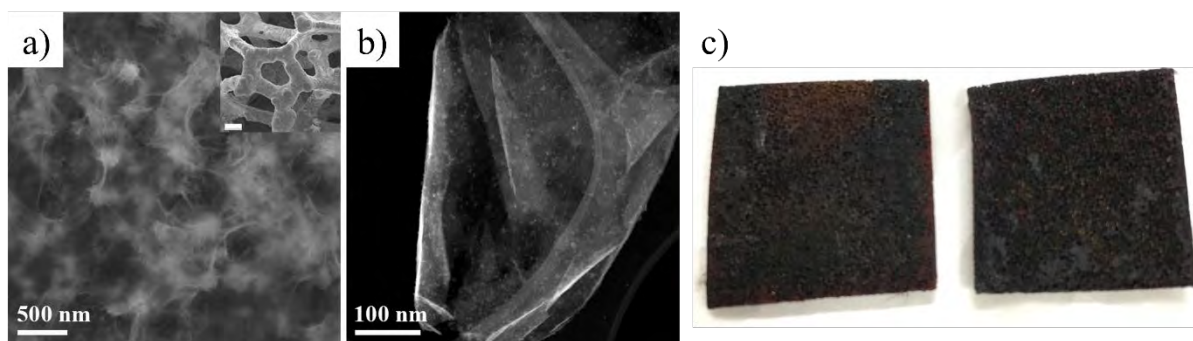


**Figure 3.** Physical characterisations and water oxidation performance of MO-based OER electrode in 1 M KOH. (a) Scanning electron microscopy images of the MO-based electrode. (b) HAADF-STEM image of MO-based catalysts obtained from the MO anodes. (c) Optical image of MO-based OER electrode.

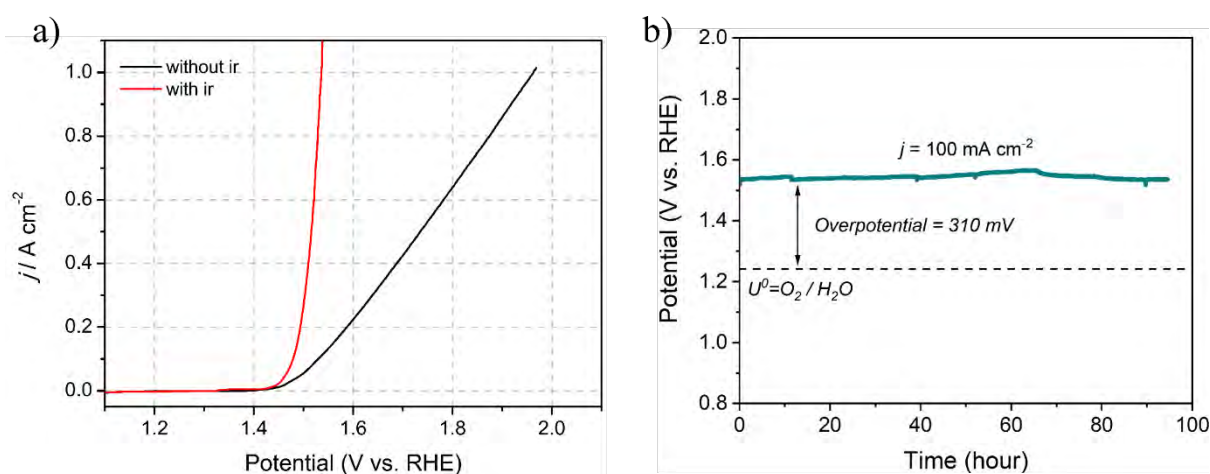


**Figure 4.** (a) Polarisation curves of MO-based OER electrode in 1 M KOH with and without  $iR$  correction. (b) Long-term durability test of MO-electrode for OER in 1 M KOH solution under a current density of  $100 \text{ mA cm}^{-2}$ .

In addition to the free-standing MO electrode mentioned above, powdery OER and HER electrocatalysts have also been developed in the Activity for advancing the ion-exchange-membrane-based electrolyser technologies that can lead to  $\text{H}_2$  production with high energy efficiencies. For instance, to tackle the cost issues associated with platinum-based catalysts for hydrogen evolution reaction (HER), Pt atomic clusters (Pt-ACs) decorated Co/N co-doped carbon (CoNC) was prepared as a cost-effective replacement. Interestingly, the Pt-ACs/CoNC exhibits an extremely high HER activity in acidic media, which is even more superior to the Pt/C benchmark under identical testing conditions. Besides that, the mass activity of Pt-ACs/CoNC is about 40 times higher than the Pt/C catalysts by the virtue of its much lower Pt loading, featuring better commercial perspectives. Mechanism investigations through physical characterisation and theoretical analysis reveal that the existence of Pt-O-Pt units in Pt-ACs/CoNC has resulted in a charge redistribution between Pt and O atoms, thus optimising the proton adsorption and hydrogen desorption on active Pt species for a high HER performance. As such,

this investigation generates valuable material design guidelines for attaining high-performance and cost effective HER catalysts in acidic electrolyte.

Besides that, constructing bi-functional electrocatalysts that can be used in a wide range of pH environment with high performance can enable the widespread application of many electrolyser devices, such as proton-exchange-membrane (PEM) and anion-exchange-membrane (AEM) electrolysers. To reduce the usage of noble metal for large-scale applications, we further developed an atomically dispersed Ru/Co dual-sites catalyst anchored on N-doped carbon (Ru/Co-N-C) for outstanding pH-universal OER and HER. Specifically, Ru/Co-N-C exhibits an ultrahigh OER and HER mass activity at a much lower loading Ru than that in commercial RuO<sub>2</sub> and Pt/C in both acid, neutral, and alkaline media, respectively. Further applying the Ru/Co-N-C catalyst in PEM water electrolysers, the device demonstrates a steady operation at an industrial-level current density. These encouraging results suggests its high atom utilization efficiency and economic feasibility. A series of experimental results and theoretical calculations reveal that the main activity centre of Ru/Co-N-C is RuN<sub>4</sub> sites. Introducing atomically dispersed CoN<sub>4</sub> sites can efficiently adjust the electronic structure and bonding strength between oxygen/hydrogen intermediate species with RuN<sub>4</sub> sites, thus achieving a high catalytical activity. Besides, the Co-N<sub>4</sub> sites can increase the electron density of Ru-N<sub>4</sub> sites, thereby improving the resistance of Ru-N<sub>4</sub> to over-oxidation and corrosion and eventually realizing a long-term stability. This work provides a new perspective for the design and synthesis of bifunctional single-atom electrocatalysts with bi- or multi-metallic active sites, especially ultralow loading of noble metals for PEM water electrolysis.

### 2.3.2 The effects of temperature and KOH concentration

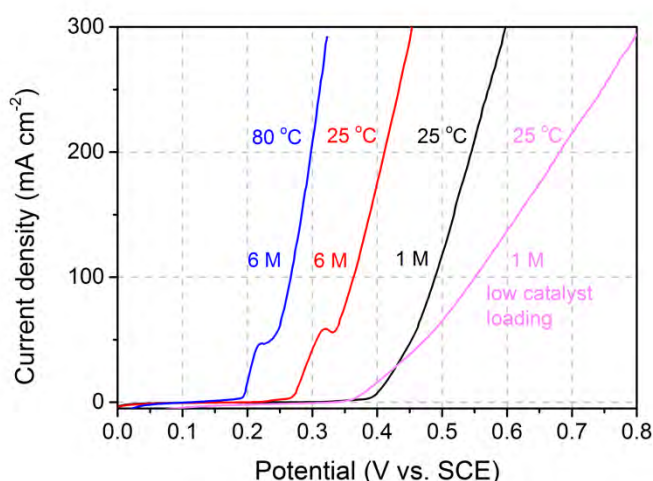


**Figure 5.** OER polarization curves of MO electrodes in alkaline media under different KOH concentrations and operation temperatures.

In this project, we also studied the effects of temperature and KOH concentration on the performances of OER electrodes. It is well known that the sluggish reaction kinetics of the anodic oxygen evolution

reaction (OER) have rendered it the bottleneck of the overall water splitting process, leading to the hydrogen production with low energy efficiencies. To further improve the OER efficiency, one effective and facile strategy is to increase the concentration of the KOH solutions. KOH solutions with higher concentrations exhibit better conductivity, which can effectively reduce the solution impedance during OER. Besides that, the higher concentration of KOH tends to provide more reactants ( $\text{OH}^-$  ions) for OER, also leading to enhanced reaction kinetics. As shown in Figure 5, the OER catalytic performance with the as-prepared MO electrode improves significantly with the increase of KOH concentration. At 25 °C, the potential required to achieve a current density of  $300 \text{ mA cm}^{-2}$  with the MO electrode has decreased from 0.6 V (vs. SCE) in 1 M KOH to merely 0.45 V (vs. SCE) in 6 M KOH, indicating obviously enhanced OER catalytic activity. Moreover, due to the endothermic nature of OER, elevating the reaction temperatures in electrolyte environment can also dramatically enhance the OER performance, thereby further reducing the overpotentials required to obtain certain current densities. As such, the as-developed MO OER electrode was further testified under different temperatures. Also displayed in Figure 5, the OER performance of the MO electrode was improved accordingly with the increase of electrolyte temperature. In the same 6 M KOH solution, the potential required to reach a current density of  $300 \text{ mA cm}^{-2}$  has decreased from 0.45 V to 0.32 V (vs. SCE) when the temperature elevated from 25 °C to 80 °C, confirming the further enhancement of OER catalytic activity. Based on the above observations, we selected 6 M KOH as the electrolyte and 80 °C as the reaction temperature for evaluating the performances the customised water electrolyzers.

### 2.3.3 The performance of customised water electrolyzers

The high-performance MO OER electrode as detailed in section 2.3.1 was assembled into a customised alkaline water electrolyser (AWE) cell to achieve high water splitting performance that can match with the power output from the CPV minimodule. As shown in Figure 6a, the customised AWE cell is mainly comprised of four components that are mechanically compressed against each other, which are: (i) a  $25 \text{ cm}^2$  MO OER electrode; (ii) a  $25 \text{ cm}^2$  NiMo-based HER electrode; (iii) a Zirfon (purchased from Agfa) gas separator; and (iv) two Ni-based current collectors engraved with flow channels. The NiMo electrode is prepared via a method reported previously, which displays a decent catalytic activity towards the HER in alkaline media. The customised AWE cell exhibits very promising performances toward the production of hydrogen. In 6 M KOH solution at 80 °C, the cell is capable of initiating the water electrolysis process at 1.35 V, corresponding to an overpotential of merely 120 mV. Apart from that, the current increases rapidly with the increase of cell voltage, reaching 2.2 A, 5 A and 9.5 A at 1.5V, 1.6 V and 1.7 V, respectively. Specifically, at 1.7V, the cell can deliver a current density as high as  $380 \text{ mA cm}^{-2}$  at an energy efficiency of 72.3%, significantly surpassing the performances of industrial alkaline water electrolysis systems. Besides that, the customised AWE cell can stably operate under 1.7 V for more than 200 hours (the test is currently ongoing in our lab), showing great promise for practical



applications. To give further insight into the role of flow channel types in improving AWE performance, the CFD modelling was also conducted, and details will be given in latter sections.

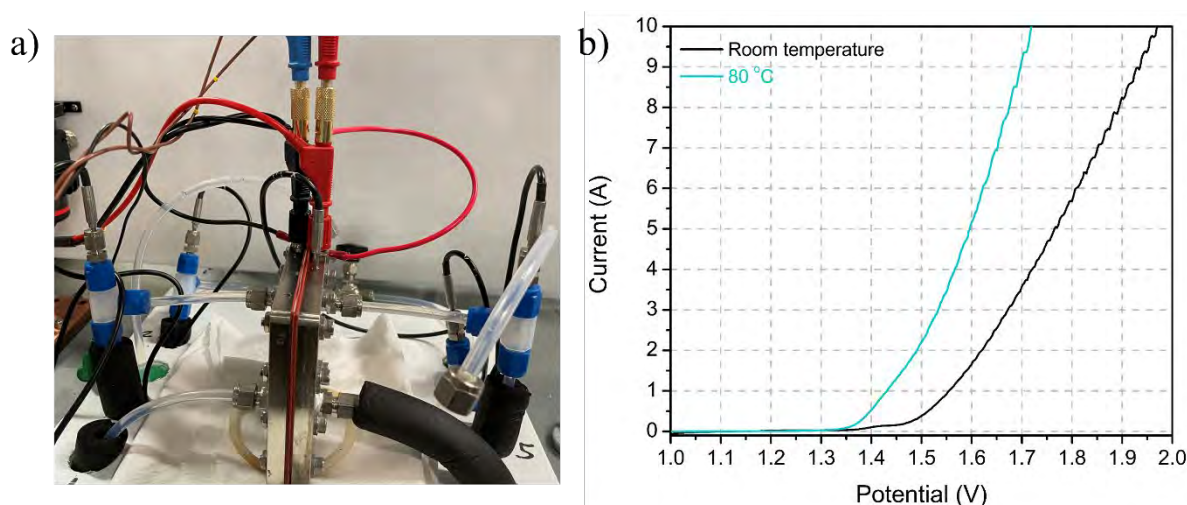


**Figure 6.** (a) Customized 20 W alkaline water electrolyser cell. (b) Water electrolysis performance using NiMo HER cathode and MO OER anode in 6 M KOH solution at a scan rate of  $5 \text{ mV s}^{-1}$ . The geometric surface area of electrodes is  $25 \text{ cm}^2$ . The polarization curves of electrolyser were operated under both room temperature and 80 degree, respectively. The inset is the optical photo image of the zero-gap electrolyser employed in this activity.

#### 2.4 Heat exchange systems

The heat exchange systems are designed and manufactured to harvest the waste heat from CPV modules to heat the electrolyser at a desired temperature for water electrolysis performance enhancements. In this project, two heat exchange systems are fabricated for the 20 W and 1 kW water electrolyser, respectively. To be specific, in the 20 W system, two water jackets connected in series (as shown in Figure 7) with an external heating source were used as both electrolyte reservoir and heat exchanger, giving a programmable temperature controlled by the heating source. The water-jacket heat exchanger was not thermally connected to CPV device in 20 W PVE system due to the limited amount of heat generated by a single cell CPV module. By contrast, in 1 kW system, an urn kettle with internal heating was customized to obtain a heat exchanger that can be thermally connected with the hot water from a 1 kW CPV module (Figure 8). The reliability of two heat exchanger systems (20 W and 1 kW) was testified for a long duration before any experiments. They are both effective in heating up the electrolyte and only take no longer than 40 minutes to achieve the target temperature. During the operation, a heat loss around 5 degrees between the temperature of electrolyte and hot water (from the external heating source) was observed in the 20 W heat exchange system, while that in a 1 kW system is around 10 degrees.



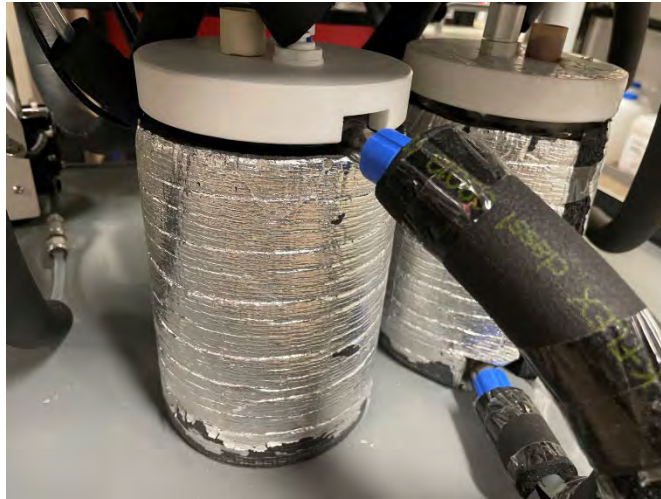


**Figure 7.** The optical photo image of the water jacket heat exchangers employed in the 20 W PVE system. The water jackets were all thermally sealed by heat insulation layers.

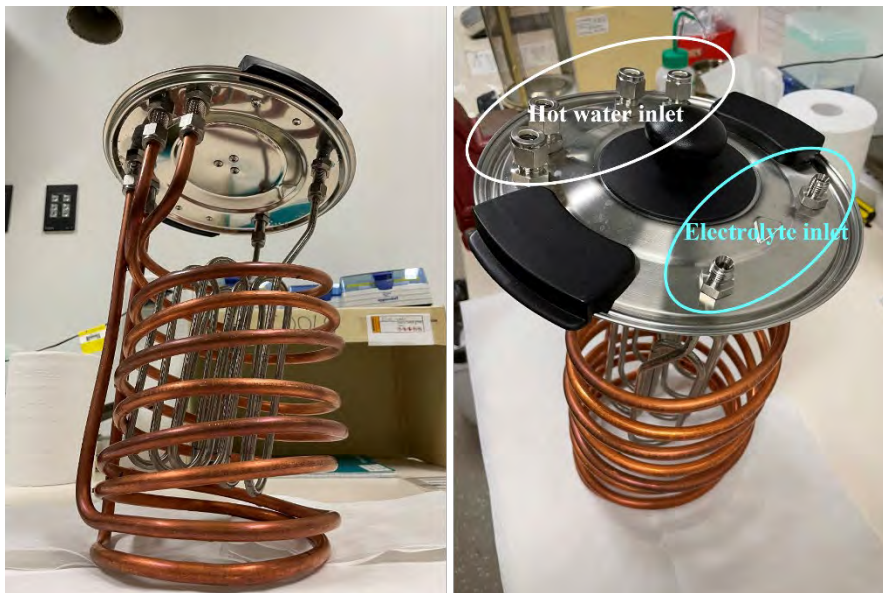


**Figure 8.** Photos of urn-based heat exchanger for 1 kW PVE systems. Hot water inlet ports were connected with the hot water loop circulated in the CPV module, while the electrolyte inlet ports were used for alkaline water electrolysis.

### 2.5 Integrated PVE systems

To electrically integrate the alkaline water electrolyzers with CPV modules in both 20 W and 1 kW PVE systems, two sets of DCDC converters were designed and developed, which convert the currents and voltages directly produced by the CPV panels to a range that can be adopted by the electrolyzers for water splitting at desirable rates. The 1 kW integrated system is assembled and measured at RayGen’s site (Figure 9, Newbridge, Bendigo, Victoria).



**Figure 9.** Photos of RayGen's CPV solar farm at Newbridge (Bendigo, Victoria).

The power source in the 1 kW PVE system is a commercial RayGen 10×10-cm<sup>2</sup> CPV module consisting of 100 high efficiency triple-junction III-V CPV cells series connected in a dense array atop a high-performance heat exchanger, where concentrated sunlight was provided by RayGen's 'solar furnace' consisting of a heliostat and parabolic mirrors (Figure 10a) to reach an intensity of 100s of suns. Upon the irradiation of concentrated sunlight, the CPV module will generate a tremendous amount of heat, which reduces its performance. Thus, to maintain an optimal operation temperature that can deliver a high STE efficiency without wasting the excessive amount of thermal energy, a pumped cooling water system was applied to the CPV module to take away the excessive amount of heat obtained from concentrated sunlight. Meanwhile, the thermal energy captured by the cooling water system can be subsequently used for heating the electrolyte through our customised heat exchanger (Figure 10d). It is worth noting that, in such a 1 kW system, the heat exchanger was thermally connected with both AWE and CPV modules to transfer the heat directly from CPV unit (e.g. ~90 °C) to heat up the electrolyte, which demonstrates the practical feasibility of using the byproduct heat in a scaled-up PVE device. To efficiently convert the currents and voltages generated by the 1 kW CPV module to a range compatible with the electrolyser, a DC-DC converter setup was built up, which includes a commercial MPPT tracker and supercapacitor 'buffer', as well as a custom DC-DC converter (Figure 10e) for the success of an efficient control of the power output from CPV module with a quick response. At RayGen's site, the temperatures and the power generated by CPV module depend greatly on the local weather, which to some extent limit the operation conditions of 1 kW PVE system. Meanwhile, the H<sub>2</sub> and O<sub>2</sub> were produced continuously at a rate that matches the CPV power.





**Figure 10.** Testing the thermally integrated 1 kW PVE system at RayGen's solar furnace testbed (July 2022): (a) Solar furnace test shed situated at RayGen's Newbridge solar farm; (b) & (c) optics to concentrate sunlight onto the CPV module; (d) thermal integration of PVE via heat exchanger; (e) operator room with DC-DC components and measurement/control computer. When illuminated, the CPV module provides both electricity and heat to the electrolyser.

Despite mostly cloudy conditions during our visit to RayGen's Newbridge, Victoria, site on 12-15 July 2022, testing of the thermally integrated 1 kW PVE system using the RayGen solar furnace during sunny periods was able to successfully demonstrate the benefits of utilising the CPV module by-product heat to heat the electrolyser, Figures 11 & 12. As shown in Figure 11, once the electrolyser was electrically powered by the CPV module (from 420 on the X axis in the top chart of Figure 11), the power of the CPV module (blue line) was adjusted efficiently by a customized DC-DC converter that matches perfectly with the power of electrolyser stacks (blue dot line).

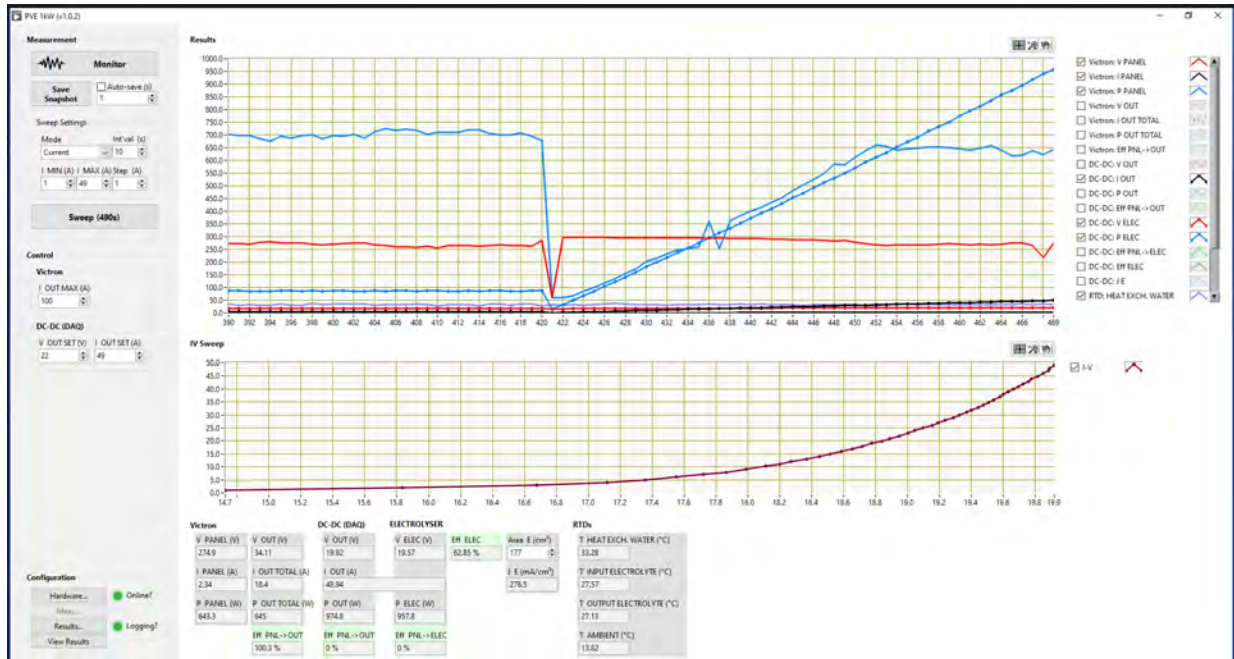


**Figure 11.** Screenshot of the measurement/control computer showing example of data during testing of the 1 kW PVE system at the RayGen solar furnace, including steady-state monitoring (top) and an I-V sweep (bottom).

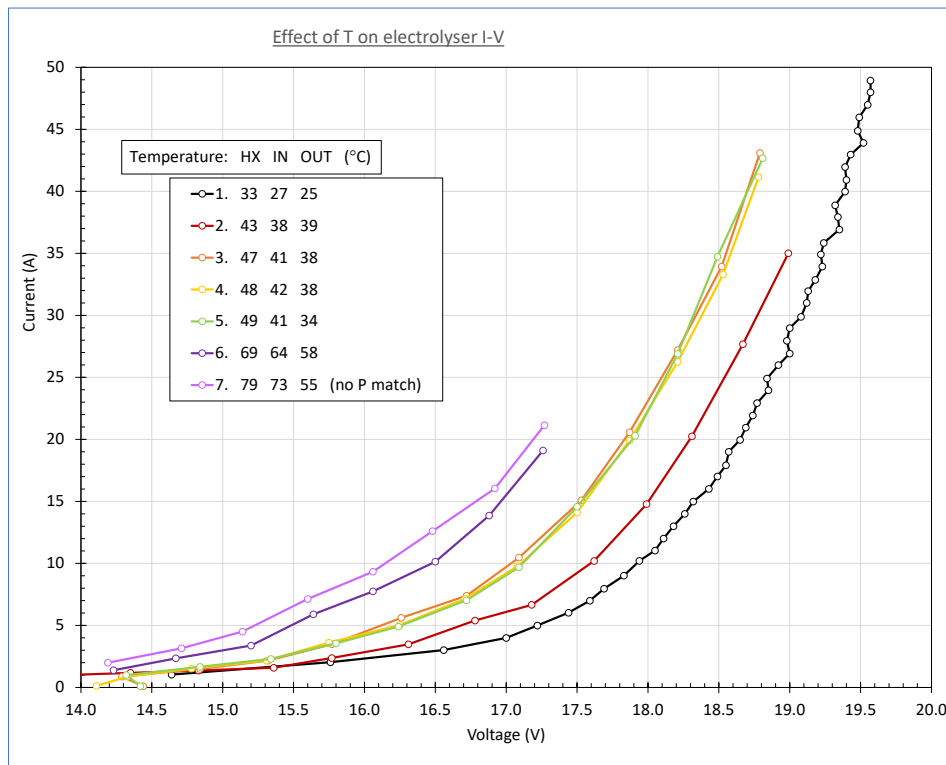


**Figure 12.** Electrolyser I-V curves measured for the 1 kW PVE system at the RayGen solar furnace. Shows the benefit of thermal integration (utilising CPV by-product heat) on electrolyser performance, namely, increased electrical current (hence  $H_2$  generation) at a given operating voltage for higher temperature electrolysis. (HX, IN and OUT represent the temperatures at heat exchanger, inlet and outlet of electrolyser stacks)



In the 20 W PVE system that was used to demonstrate a high STH efficiency, the photovoltaic electricity generated by the CPV minimodule was directly connected with the electrolyser cell through a DC-DC converter, and the currents and voltages applied on the water electrolyser were monitored by a data acquisition system (based on LabView program, Figure 13). Owing to the power limit of the CPV minimodule (up to 11 W), the thermal energy required to heat the electrolyte to the target temperature is provided by a hot water bath as external heating source. Meanwhile, the CPV cell was maintained at 25°C by a separate cooling water bath to guarantee a high solar to electricity efficiency (> 38%). As shown in Figure 13b, through a customized DC-DC converter, the electricity generated from the CPV minimodule can be efficiently used to power the 20 W water electrolysis process. After the conducting the indoor reliability test, the 20 W PVE system was employed for outdoor measurements under natural sunlight (Figure 14). With a solar tracker, the 20 W PVE system was operated under the maximum power point (MPPT) to deliver a high STE efficiency to guarantee a superior STH efficiency that is further supported by the high water electrolysis performance in the MO-anode-based electrolyser cell. Under a potential of  $\sim 1.55$  V (corresponding to a water electrolysis efficiency of 79.3 %), the electrolyser performance can perfectly match with that of CPV device at its MPPT, giving a STH efficiency as high as 28.9 % (25.9% including the lead losses), which is one of the highest under such catalytic current ( $242 \text{ mA cm}^{-2}$ ).

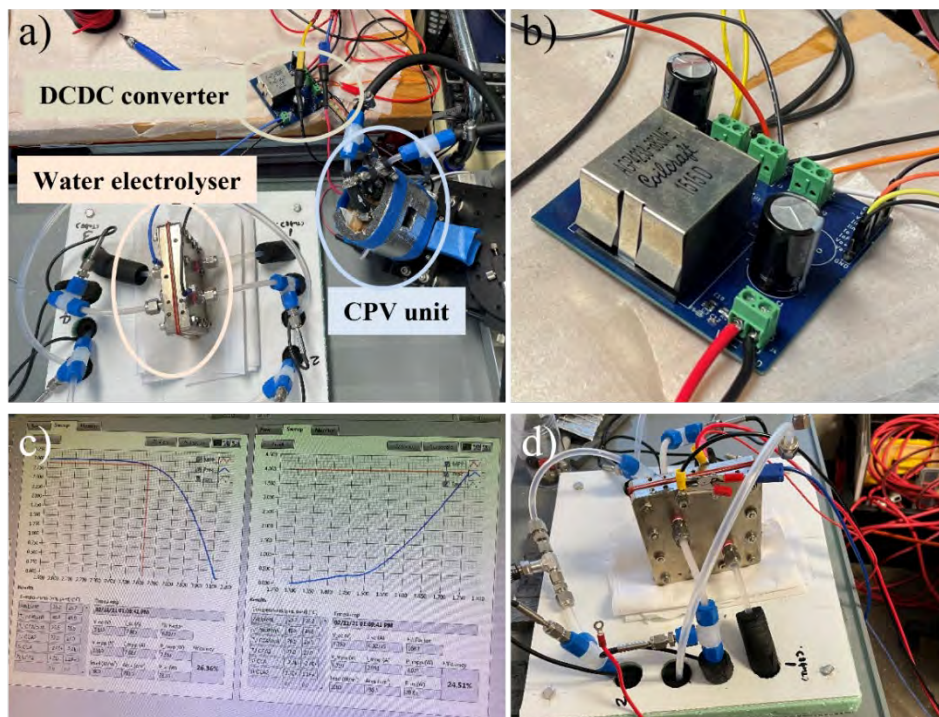


**Figure 13.** Optical photo images of the integrated 20 W PVE system. Photo image of (a) indoor PVE test using the integrated 20 W PVE setup, (b) customized DCDC converter, (c) LabView program and (d) 20 W alkaline water electrolyser cell.

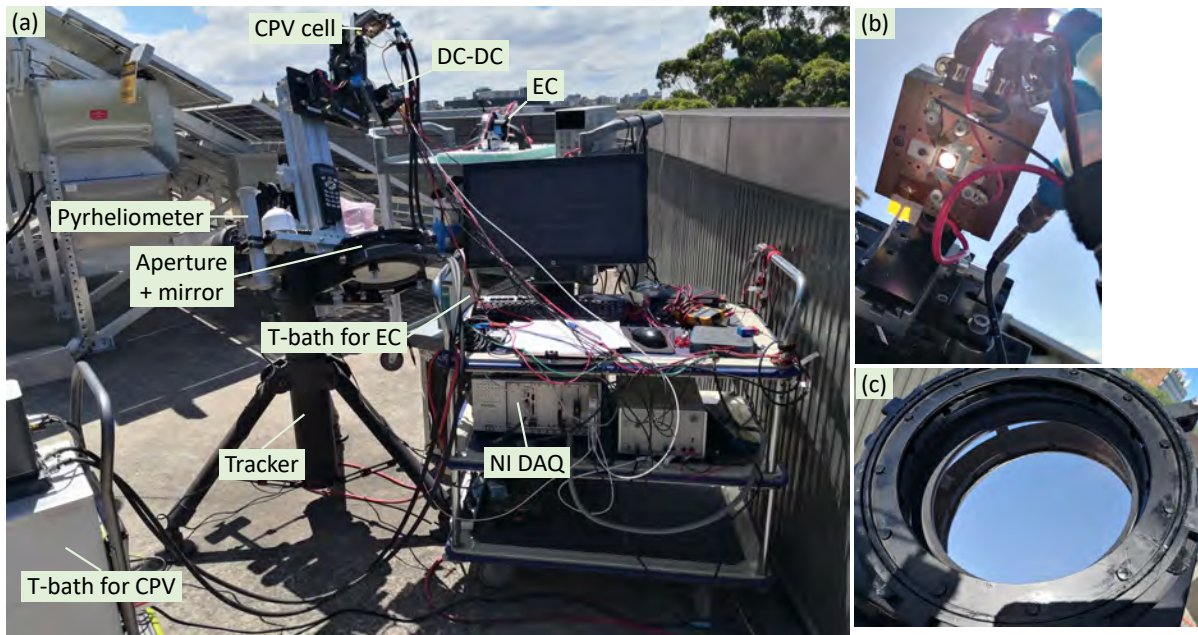


**Figure 14.** (a) 20 W PVE system during outdoor testing at UNSW. Note the proximity of the CPV cell, DC-DC converter & electrolyser cell (EC) to minimise lead  $I^2R$  resistance losses, the use of separate temperature controlled baths for CPV (to maintain cell at 25 °C) and EC (to maintain EC at 80 °C), and use of iris aperture in front of the concentrating mirror to control sunlight concentration (< 500 suns); closeups of (b) CPV cell on heatsink (the white spot is the illuminated area on the 1-cm<sup>2</sup> CPV cell), and (c) concentrating mirror with custom-made & fitted iris aperture.

During outdoor tests of the 20 W PVE system, data were saved at 5 second intervals, full aperture I-V sweeps were regularly performed to determine CPV cell  $I_{sc}$  and irradiance calibration values, and at each aperture setting (which controls the sunlight concentration) an I-V sweep was performed then the pulse width modulation (PWM) duty cycle (which controls the voltage output of the DC-DC converter) was optimised for maximum STH efficiency. At a given aperture setting and having maximised the STH efficiency, we then ‘hold’ the PVE system at these conditions for periods of 5 to 20 minutes to demonstrate performance stability – see Figure 15&16 below.



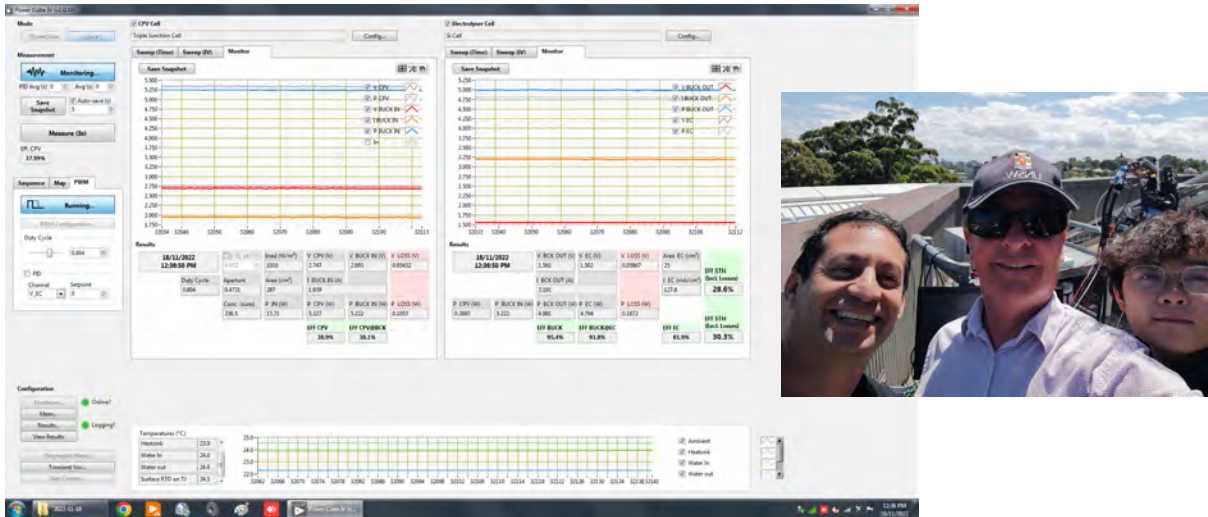


**Figure 15.** Screenshot of the 20 W PVE system measurement/control software, showing example data obtained during outdoor testing at UNSW (18 November 2022). Inset shows team members (left to right) Ivan Perez-Wurfl, Mark Keevers & Yihao Shan after a successful outdoor test session.

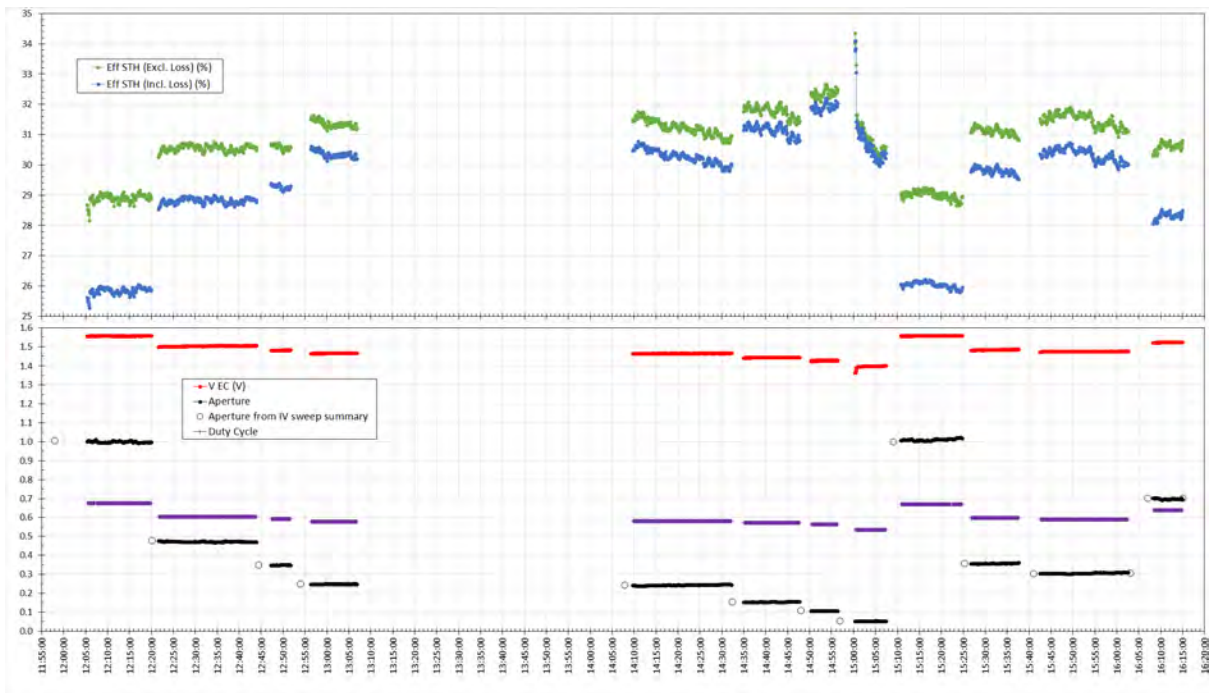


**Figure 16.** Time series data (5 second intervals) for key parameters of the 20 W PVE system measured during outdoor testing at UNSW (18 November 2022). The data has been filtered to show just the values during aperture & PWM duty cycle ‘hold’ periods (typically 5-20 minutes duration). Note that the STH values are raw, prior to correction.

The STH efficiency is corrected by a scaling factor, as per below equation:

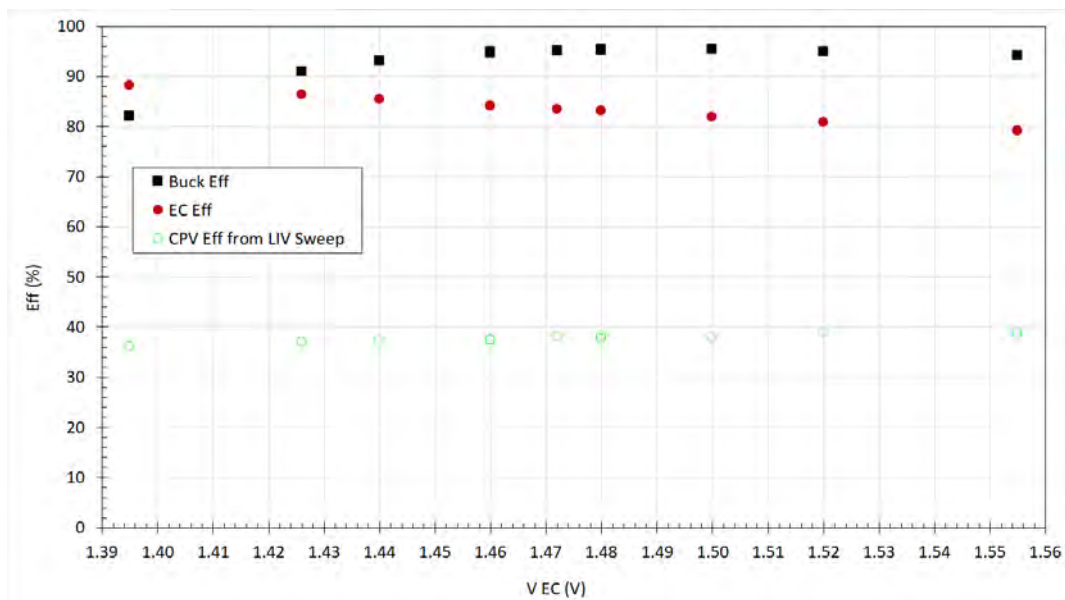
$$\text{Scaling Factor} = \frac{\text{Efficiency of CPV from LIV Sweep prior to HOLD}}{\text{Efficiency of CPV from ave. Monitor values at HOLD}}$$

And that,

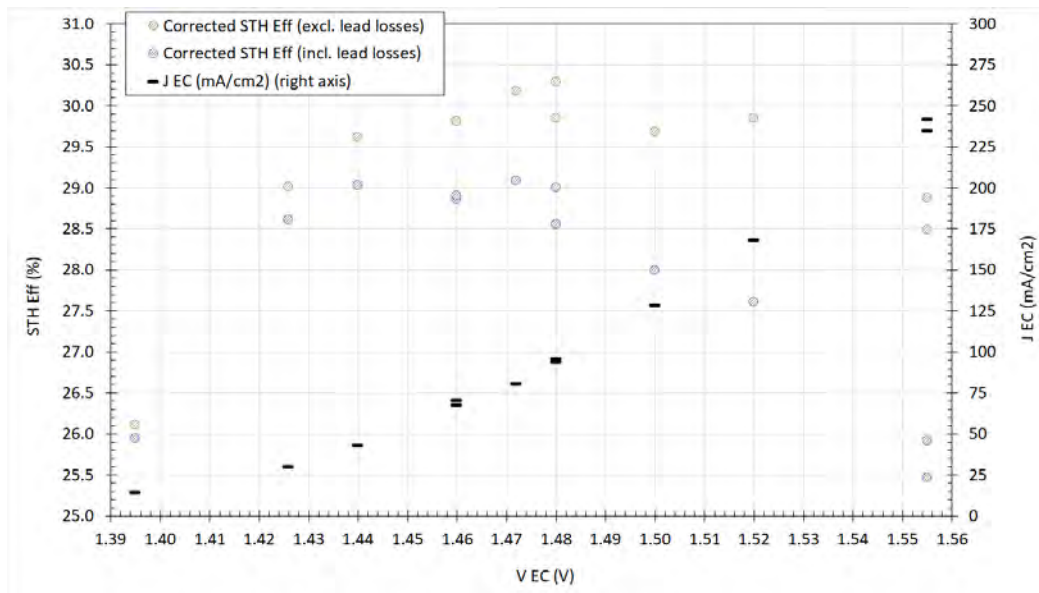
$$\text{STH Eff excl lead } I^2R \text{ losses} = \text{CPV Efficiency} \times \text{Buck Efficiency} \times \text{EC Efficiency}$$

Note that we are in the process of recalibrating the I and V measurements in the 20W PVE Systems, so these Efficiency results are tentative. More accurate results will be obtained prior to peer-review publication.

We have demonstrated a peak STH efficiency (excluding lead losses) of 30.3% (29.1% including the lead losses) near the thermo-neutral voltage of 1.47 V with electrolyser current density ( $J_{EC}$ ) of 80 mA/cm<sup>2</sup> – see Figure 17 below. In the near term, we anticipate improving the STH efficiency by further reduce  $I^2R$  losses by shortening the lead lengths between the CPV cell, DC-DC converter and the electrolyser cell, as well as by swapping out the triple-junction CPV cell for a higher performance 5-junction CPV cell.



(a)



(b)

**Figure 17.** Measured outdoor results for the 20 W PVE system, with CPV and EC units operated at 25 and 80 °C, respectively. (a) Efficiencies of the three key components (DCDC converter, electrolyser and CPV) versus electrolyser voltage (1.47 V is adopted here as the thermoneutral voltage); and (b) overall solar-to-hydrogen (STH) conversion efficiencies versus EC voltage, with or without lead  $I^2R$  power losses, and the corresponding EC current densities (right axis).

## 2.6 CFD modelling

A VOF-based three dimensional transient CFD model is developed to study the two-phase flow behaviour in the water electrolyser's flow channel. The model is first validated against the experimental results in terms of single bubble evolution in a bubble column [2] and two-phase flow regime in an electrolyser flow channel [3], as shown in Figure 18. The validation results showed that this VOF-based CFD model is capable of capturing the bubble evolution in an electrochemical process.

After that, this model is utilised to study the two-phase flow behaviour in three existing flow channel designs, *i.e.*, single serpentine, parallel, and pin, in terms of electrolyte flow velocity (Figure 19 a-d), bubble quantification (Figure 19e), volume of hydrogen exited (Figure 19 f), and pressure drop (Figure 19 g). Based on the CFD simulation results, the flow channel with higher flow velocity has a higher pressure drop. High flow velocity can promote the bubble removal, however, high pressure drop can cause stress distributions on electrolyser components and electrolyte leakage. The trade-off between efficiency and durability of the electrolyser is achieved by proposing a novel flow channel design, *i.e.*, parpentine, to lower the pressure drop while maintaining the bubble removal rate. Parpentine design combined both the features of single serpentine design and parallel design. The CFD simulation results of the parpentine design showed that it has a significantly lower pressure drop than single serpentine and more even electrolyte distribution than parallel and pin.

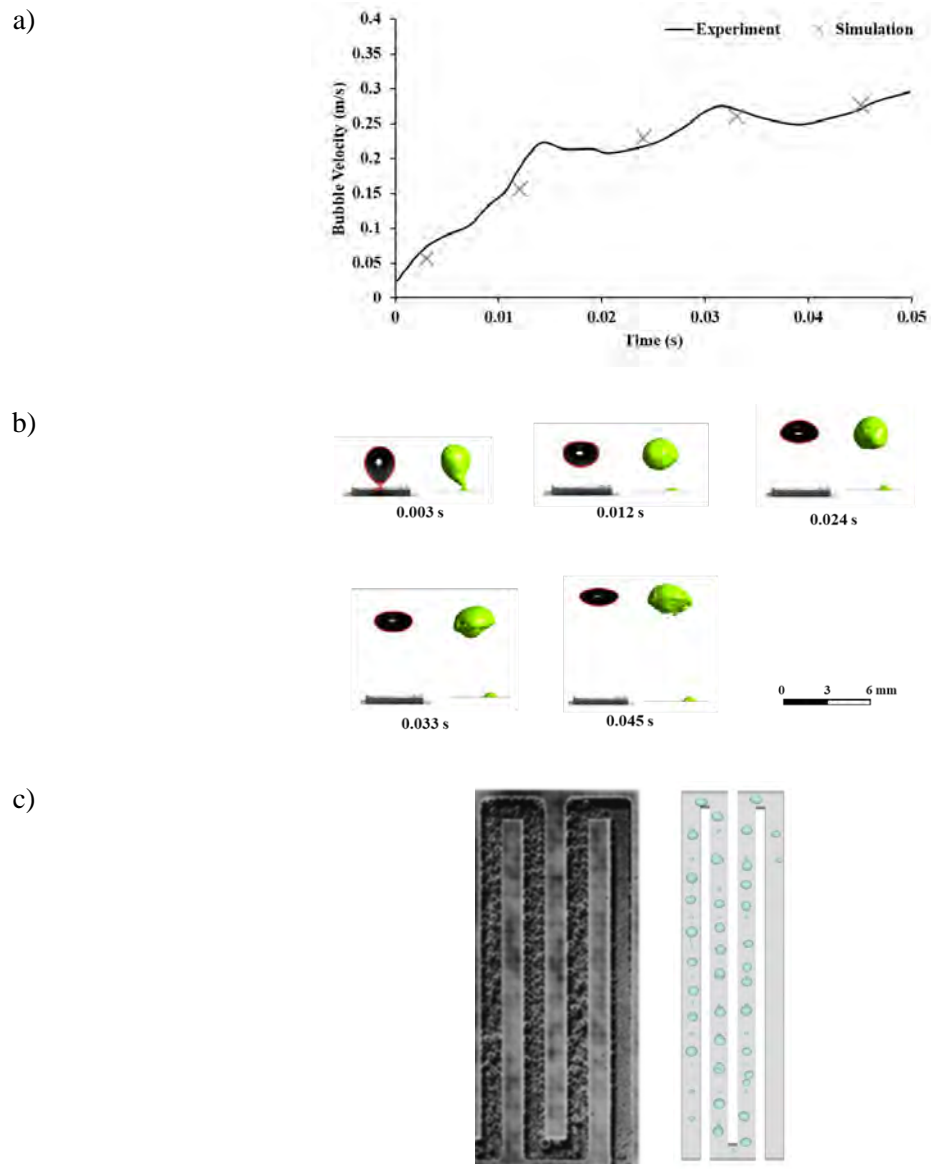


**Figure 18.** Model validation of bubble evolution in terms of (a) bubble velocity and (b) bubble shape of a single bubble evolution measurement in Ref. [2], and (c) two-phase flow regime in an electrolyser flow channel in the simulation (right) against the snapshot in the electrolyser experiment [3] (left).

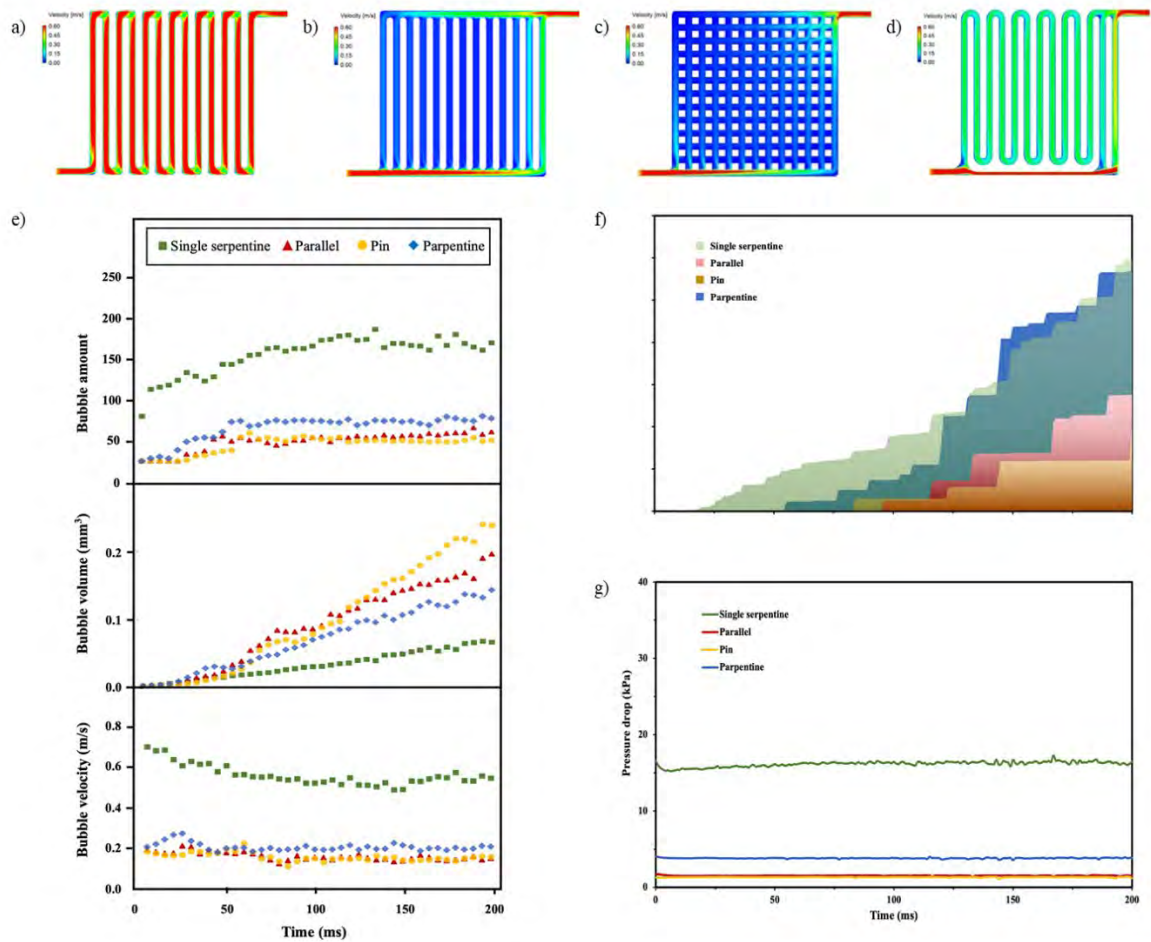


**Figure 19.** Two-phase flow behaviour in different flow channel designs. Electrolyte flow distribution in a) single serpentine, b) parallel, c) pin, and d) parpentine. e) The bubble amount, average bubble volume, and average bubble velocity along the simulation time in the flow channels. f) The cumulative volume of hydrogen exited from the flow channels along the simulation time. g) Pressure drop along the flow channels.

## 2.7 Techno-economic analysis

Technoeconomic modelling utilising tools developed and vetted through industry consultation via the HySupply and NSW Power to X Feasibility Study Projects<sup>1</sup> were carried out for scaled-up (100 MW, 500 MW and 1 GW) solar PVE system. The performance data were taken from experimental results and assumed to be replicated at the large-scale capacities modelled. Further details on the modelling assumptions can be found in **Table 1**. Our modelling results (summarised in **Table 2**) indicate that through deployment of the developed PVE system through this ARENA grant, the levelised cost of hydrogen ( $LC_{H_2}$ ) can be reduced from \$9.13/kg to \$6.66/kg (for 100 MW system), \$8.52/kg to \$6.22/kg (for 500 MW system) and \$8.29/kg to \$6.05/kg (1 GW system) assuming current capital costs of \$1400/kW for 1 MW modules (2022 pricing) and modelled for 24% capacity factor in northern and western region of Australia.

<sup>1</sup>(<https://www.globh2e.org.au/hysupply-cost-tool>)



While cost of electrolyzers are expected to organically decrease over the years, which would lead to significant decrease in  $LC_{H_2}$ , our results overall highlight the benefit of our combined heat and PVE system in drastically decreasing  $LC_{H_2}$  by at least 25%, presenting a pathway for commercialisation of the system.

**Table 1. Operating and cost parameters assumptions for the room temperature electrolysis and high temperature electrolysis scenarios.**

Parameter	Assumptions		Reasoning
	Room Temp. Electrolysis	High Temp. Electrolysis	
<b>Electrolyser System</b>			
<b><u>Operating Parameters</u></b>			
Efficiency	55 kWh/kg (60% LHV) [4]	40 kWh/kg (83% LHV) [4]	Based on data collected from pilot scale project.
System Load Range	10 – 100%	10 – 100%	Based on commercial AE electrolyser systems (Aurecon <sup>1</sup> and AEMO, 2020) <sup>2</sup>
Stack Lifetime	60,000 hrs	60,000 hrs	Based on commercial AE electrolyser systems [4]
Stack Degradation	1%/year	1%/year	Based on commercial AE electrolyser systems [4]
Water Requirement	15 L/kg [4]	20 L/kg [4]	Increased by 30% to account for cooling requirements
<b><u>Cost Parameters</u></b>			
Installed Electrolyser Cost	A\$1,400/kW at 1 MW Scale		Based on commercial AE electrolyser systems [5] <sup>3</sup>
Economies of Scale	Scale Index Model assuming scale factor of 0.9		Based on literature suggested scale factor [6]
Land Cost	8% of Electrolyser Installed Cost		Based on commercial AE electrolyser systems [4]
O&M Cost	2.5%/year [4]	5%/year [4]	Doubled to account for high temperature operation leading to more frequent maintenance needs.
<b>Concentrated Solar Thermal System</b>			
<b><u>Operating Parameters</u></b>			
Degradation Rate	0.2%/year		Based on commercial CST systems [4]
<b><u>Cost Parameters</u></b>			
CST System Equipment Cost	A\$1,100/kW Electricity Supply Cost – A\$150/MWh (For 100% capacity factor operation)		Based on data provided by RayGen.

<sup>1</sup> Aurecon, AEMO, 2020. 2020 Costs and Technical Parameter Review.

<sup>2</sup> AEMO, 2018. AEMO costs and technical parameter review Report Final Rev 4 9110715

<sup>3</sup> Graham, C., Hayward, P., Foster, J., Havas, L., 2022. GenCost 2021-22.



CST System Capital Cost Breakdown	75% Equipment Cost/25% Installation Cost	Based on commercial CST systems [4]
Land Development Cost	4% of CST System Capital Cost	Based on commercial CST systems [4]
CST System O&M Cost	2% of CST Capital Cost/year	Based on commercial CST systems [4]
<b>Electrolyser – CST Powerplant Integration Costs</b>		
Interconnection Costs – Piping	2.5% of Electrolyser Capital Costs	Stakeholder input
DC/DC Convertor Costs	5% of CST System Powerplant Costs	Based on commercial utility scale PV systems in Australia [7]
Pump	1% of Total Equipment Costs	Stakeholder input
Heat Exchangers	1% of Total Equipment Costs	Stakeholder input
<b>Financing Parameters</b>		
Discount Rate	7%	Based on renewable energy projects in Australia [8]
Project Life	25 Years	Based on commercial CST systems/Electrolyser System [4]

**Table 2. Summary of cost reduction based on proposed high temperature electrolysis system.**

Parameter	Low Temp. Electrolysis		High Temp. Electrolysis	
	Solar limited Capacity factor	100% Capacity Factor (firmed using CPV)	Solar limited Capacity factor	100% Capacity Factor (firmed using CPV)
<b>100 MW System</b>				
LCOH (A\$/kg <sub>H2</sub> )	<b>9.13</b>	<b>10.29</b>	<b>6.66</b>	<b>7.50</b>
Investment Required (A\$)	261 million			
<b>500 MW System</b>				
LCOH (A\$/kg <sub>H2</sub> )	<b>8.52</b>	<b>10.12</b>	<b>6.22</b>	<b>7.38</b>
Investment Required (A\$)	1.23 billion			
<b>1 GW System</b>				
LCOH (A\$/kg <sub>H2</sub> )	<b>8.29</b>	<b>10.05</b>	<b>6.05</b>	<b>7.33</b>
Investment Required (A\$)	2.41 billion			

A key advantage of coupling RayGen’s CPV system with the electrolyser is the additional flexibility of operating the electrolyser beyond the 24% capacity factor afforded by solar irradiance by using stored energy to allow for 100% capacity factor operation. The 100% capacity factor will allow 24/7 operation, which is critical for using renewable hydrogen and converting to useful derivatives such as ammonia and methanol, conversion processes that require steady-state operation and hence constant hydrogen supply. At present, renewable intermittency presents a challenge to profitably run ammonia and methanol facilities and where expensive storage systems such as battery, hydrogen storage as well as reusing generated hydrogen to power the electricity generation are still required.

The LCOH breakdown for low-temperature and high-temperature electrolysis with the PVE system run at both 24% capacity factor and 100% capacity factor is presented in the figures on the following pages (**Figures 20 – 22**)

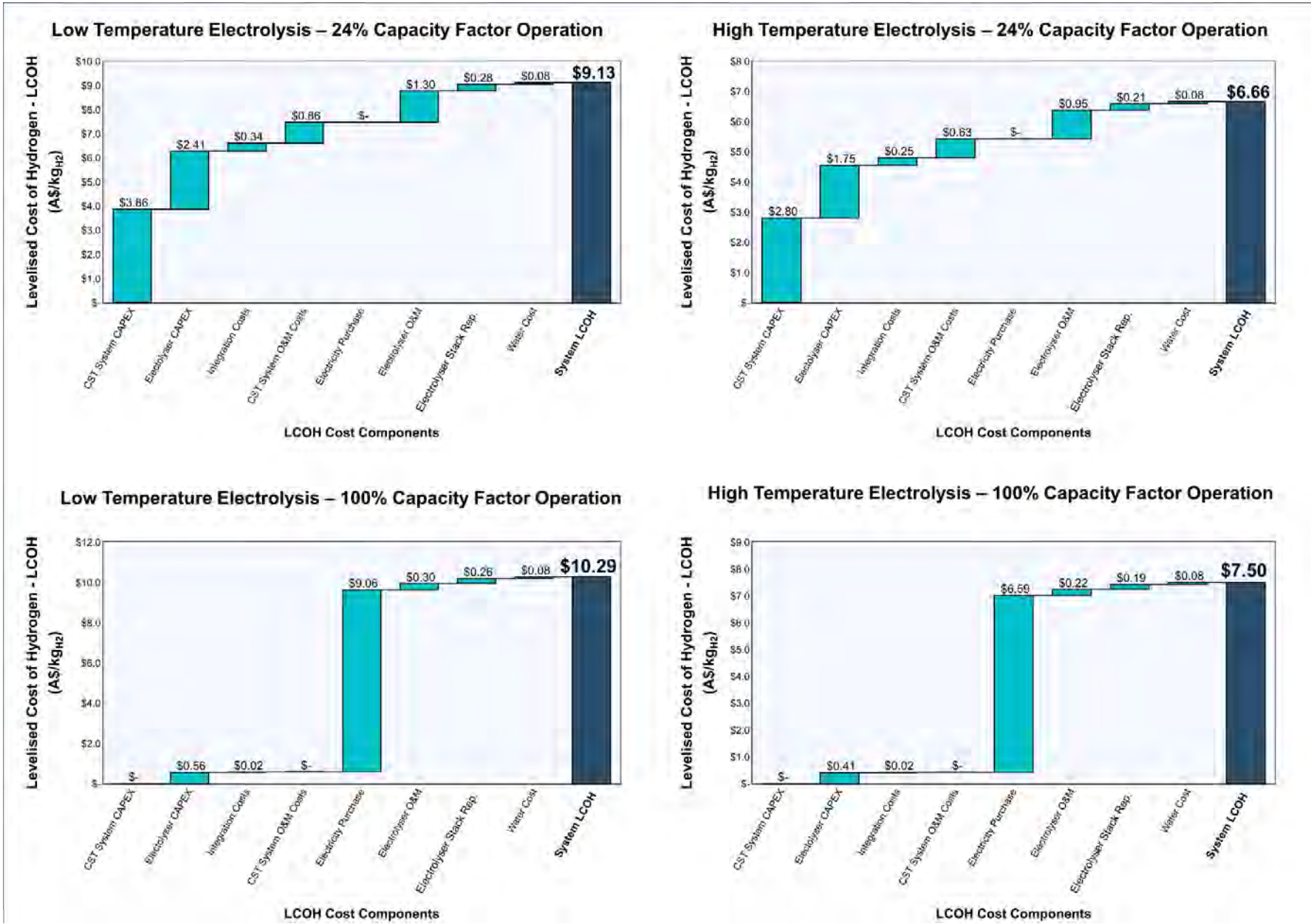


**Figure 20.** Levelised Cost Breakdown of the Low Temperature Electrolysis vs High Temperature Electrolysis at 100 MW scale.

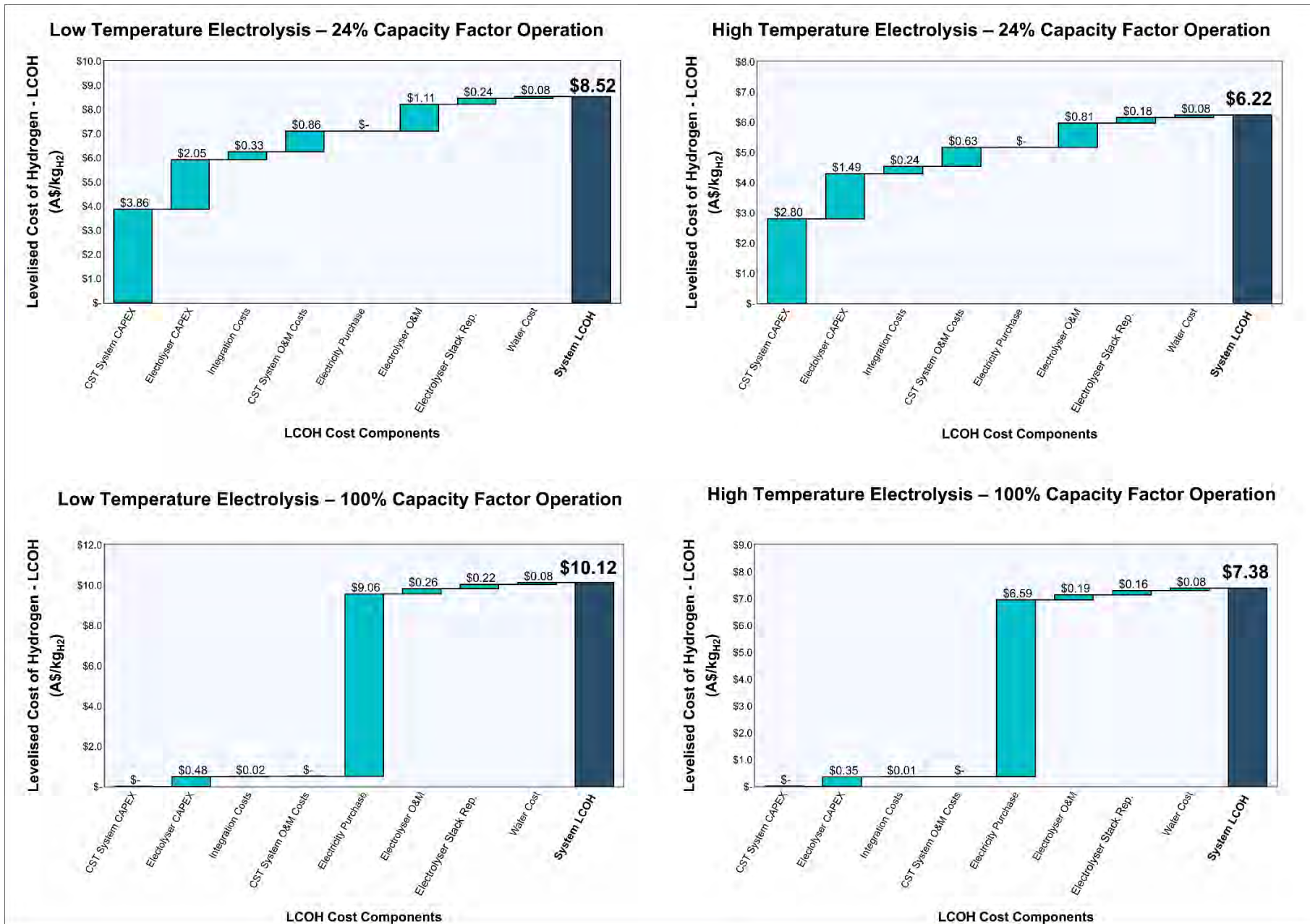
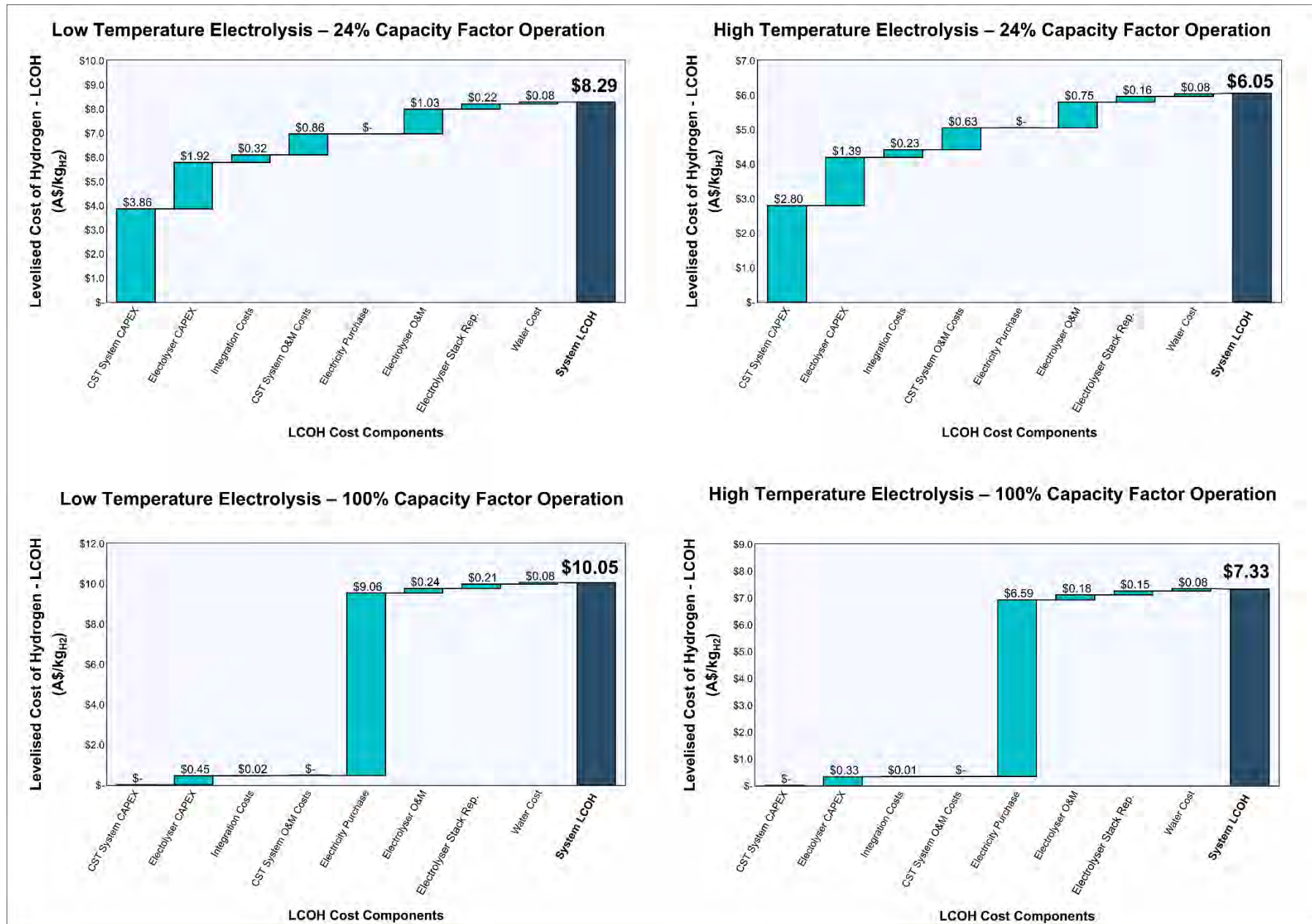


Figure 21. Levelised Cost Breakdown of the Low Temperature Electrolysis vs High Temperature Electrolysis at 500 MW scale.





**Figure 22.** Levelised Cost Breakdown of the Low Temperature Electrolysis vs High Temperature Electrolysis at 1 GW scale.

### 3. Challenges Encountered and Lessons Learned

#### 3.1 Water electrolyser cell

**(i) Challenges:** Firstly, the water electrolysis performance changes drastically upon the overall resistance of electrolyser, which depends largely on the cell configurations. The electrolyser employed in this activity is a zero-gap alkaline water splitting cell including electrodes, gas separator, current collectors and gaskets that were all compressed against each other. The thickness of separator determines the ion-exchange resistance between anode and cathode, thereby necessitating the adoption of ultrathin separator membranes for a low resistance. However, thin membranes normally make the alignment of each cell component difficult, as it may not be able to withstand the mechanical compression between anode and cathode that generally sandwiches the gas separator. Thus, the adoption of ultrathin membranes with a robust mechanical strength is highly desired in assembling a high-performance water electrolyser cell.

Secondly, a compact electrolyser structure is generally required for decreasing the cell resistance and achieving a good sealing of electrolyte. Nevertheless, such a compact structure may also increase the bubble diffusion resistance in gas diffusion channels due to the highly compressed alignment of each component, thereby building up gas and pressure in the electrolyte chamber and subsequently decreasing the contact between electrolyte and catalysts that leads to a low performance. As such, effective strategies would be important to achieve both low electrical resistance and gas diffusion resistance in electrolyser structure.

**(ii) Resolutions:** To tackle the above issues, we have purchased the newly released ultrathin Zirconium-based gas separators ( $\sim 50 \mu\text{m}$ , Zirfon) with a high mechanical strength, which is used in both 20 W and 1 kW electrolysers. The Zirfon separators can withstand the strong compression between anode and cathode without any membrane penetration/distortion and possible short circuit. This leads to an extremely low cell resistance ( $<1 \Omega$ ) of the as-assembled electrolysers. The gas diffusion condition in electrolyser was then optimized by employing porous self-standing electrodes on both anode and cathode side. The Ni-foam-based electrodes provide not only abundant open pores for a fast mass transport (e.g.  $\text{O}_2$ ,  $\text{H}_2$  and electrolyte) but also a mechanical support to withstand the strong compression without blocking the gas diffusion channels.

#### 3.2 Accurate control and monitoring of temperature

**(i) Challenges:** Accurately controlling the electrolysis temperature requires the ability to precisely monitor the temperatures at important cell components. In this regard, resistance temperature detector (RTD) sensors with a rapid temperature response were used to detect the temperatures in both electrolyte (outlet) and metallic current collectors. However, the gas/electrolyte mixture contains numerous fine bubbles would significantly influence the data collection accuracy of RTD as it suffers



from frequent contact with both electrolyte and gas, which exhibits different temperatures due to their difference in heat capacity.

**(ii) Resolutions:** To accurately monitor the electrolysis temperature, commercial RTD sensors were modified with a customized T connection shell (Figure 6a) at the electrolyte inlet pipe to avoid the accumulation of gas bubbles at the RTD surface. Meanwhile, another digital RTD was attached on the surface of the metallic current collector to monitor the temperature of cell when the electrolysis conditions reach steady state. In this case, an accurate monitoring of electrolysis temperature could be achieved when both electrolyte temperature and cell temperature reach steady-state.

### *3.3 Electrical integration between CPV and AWE*

**(i) Challenges:** Perfectly matching the power between CPV and AWE modules is challenging due to the different ranges of current and voltage required to achieve an ideal performance under high efficiency for these two devices. Normally the voltage generated by the CPV module is lower than that required by AWE device at desirable rates (e.g.  $> 1.5$  V), while the photovoltaic currents produced by CPV at specific potentials are higher than that required by water electrolysis. To this end, perfectly matching the power between CPV and AWE units is urgently required but still challenging, especially for the 1 kW system with a high-power output.

**(ii) Resolutions:** In 20 W system, to match the power between CPV module and water electrolyser, a customized DCDC converter board was designed and fabricated (Figure 13b), which exhibits a conversion efficiency higher than 98%. The electrical leads between DCDC converter and either the electrolyser or the CPV device were made as short as possible to maintain a low charge transfer resistance. In addition, a slightly more complicated DCDC converter system was assembled for the 1 kW system with the assistance of a MPPT tracker and a supercapacitor (Figure 10e).

## **4. Commercialisation Prospects**

*Primary project outcomes:*

Throughout the lifespan of this project, we have attained the following outcomes:

- PVE prototypes that demonstrate a high STH efficiency up to 30% and practical feasibility of scaling up to generate green H<sub>2</sub> in large scale.
- High-performance water oxidation anodes for efficient water electrolysis in alkaline media.
- Customised heat exchangers to efficiently harvest the heat from CPV modules to increase the temperature of electrolyte in electrolysers.
- Customised DC-DC converter to match the output of CPV with the input of water electrolysers with high energy efficiency ( $>95\%$ ). Progression of activity from TRL3 to TRL4 over the course of the project.

- A Solar-to-Hydrogen (STH) conversion efficiency of around 30% successfully achieved
- Levelized cost of H<sub>2</sub> down to 6.66 AUD/kg when the system is scaled up to 100 MW.

*Pathway to commercialization:*

The current technology is at TRL4. Over the next three years, our focus will be on adapting the technology to produce customised electrolyser single stacks with a capacity of 5 kW, and electrolyser stacks that can reach MW scale for practical applications. To achieve this, we plan to establish a close collaboration with leading electrolyser manufacturing companies, leveraging their expertise and resources to help us achieve the goals. By the end of this three-year period, we aim to advance our technology to a higher TRL level (TRL6 or TRL7), and to make significant progress towards the commercialisation of our electrolyser technology.

## 5. Knowledge Sharing Activities

The following lists the activities undertaken and outputs arising from the Activity:

### 5.1. Events/Activities/Outreach

#### 2022

- A video explainer on how the highly integrated PVE system for renewable hydrogen production is available on [Highly Efficient & Low Cost Photovoltaic-Electrolysis System](#)



- A video of Dr Ivan Perez-Wurfl on ‘Unleashing the power of solar energy’ published by UNSW Centre for ideas mentioned about this ARENA project (Ivan as collaborator) and the concept of

utilising the byproduct heat from the CPV system to improve electrolyser hence increase hydrogen production efficiency: <https://www.centreforideas.com/article/ivan-perez-wurfl-unleashing-power-solar-energy>

- CI Lu attended the 2022 International Symposium on Clean Energy Materials in Gold Coast as an invited speaker.
- CI Lu attended the 4th International Conference on Emerging Advanced Nanomaterials (ICEAN) in Newcastle as an invited speaker.
- CI Lu presented the ARENA results in International Workshop on Emerging Energy Materials and Technologies for Carbon Neutralization (online) organised by Shanghai University.
- CI Amal presented ARENA project as part of the technology showcase during meeting with Rio Tinto Office of Chief Scientist Team visit to UNSW in June 2022.
- PhD student Xiaoying Wong presented work during the research showcase session at the launch of the ARC TC for the Global Hydrogen Economy, 5 December 2022
- PhD student Chengli Rong presented findings from ARENA project at RACI 2022 National Congress in Brisbane, 3 – 8 July 2022
- PhD student Chengli Rong presented findings from ARENA project at Hydrogen Storage and Production Conference, 20 – 21 Oct 2022 at UNSW

## **2021**

- CI Lu presented the ARENA project: Efficient Solar to Hydrogen Conversion Process enabled by Photovoltaic Electrolysis at Energy Future Conference (virtual conference), 18 – 21 Oct 2021
- CI Amal presented at Applied Nanotechnology and Nanoscience International Conference – ANNIC 2021 (virtual conference), 24<sup>th</sup> – 26<sup>th</sup> March 2021

## **2020**

- CI Lu attended the International Conference on Energy and Environmental Materials 2020 (EEM2020) in Gold Coast as an invited speaker.
- CIs Lu and Amal attended the 8th International Conference on Nanoscience and Nanotechnology (ICONN 2020) in Brisbane as an invited speaker and a Plenary Speaker.

## **2019**

- CI Lu attended the 1st International Conference on Clean Technologies for a Blue Planet in Gold Coast as an invited speaker.
- CI Lu attended 18th Asian Pacific Confederation of Chemical Engineering Congress in Sapporo to present the work on OER catalysts.
- CI Lu attended a series of workshops held in Shanghai Jiaotong University and Zhejiang University to disseminate the findings within this project.

- PhD student Qingran Zhang presented his work on ‘Fully reversible water electrolyser cell’ at nanoGE Fall meeting in Berlin Germany, 6 Nov 2019
- CI Amal presented ARENA project findings to the Mitsubishi Heavy Industries group visiting UNSW in August 2019 to explore opportunity for potential collaboration with MHI and UNSW
- CI Amal presented at ICMAT 2019, Singapore as a Keynote Speaker

## 2018

- CI Amal presented ARENA project in the meeting with Woodside Group visiting UNSW in August 2018 exploring expertise on Hydrogen and opportunities for research investment by the group.

## 5.2 Publications

### Published

- (1) Y. Zhao, P. V. Kumar, X. Tan, X. Lu, X. Zhu, J. Jiang, J. Pan, S. Xi, H. Y. Yang, Z. Ma, T. Wan, D. Chu, W. Jiang, S. C. Smith, R. Amal, Z. Han, X. Lu, Modulating Pt-O-Pt atomic clusters with isolated cobalt atoms for enhanced hydrogen evolution catalysis, *Nat. Commun.*, 13, 2430 (2022).
- (2) C. Rong, X. Shen, Y. Wang, L. Thomsen, T. Zhao, Y. Li, X. Lu, R. Amal, C. Zhao, Electronic Structure Engineering of Single-Atom Ru Sites via Co-N<sub>4</sub> Sites for Bifunctional pH-Universal Water Splitting *Adv. Mater.*, 34, 2110103 (2022).
- (3) Z. Tian, Q. Zhang, L. Thomsen, N. Gao, J. Pan, R. Daiyan, J. Yun, J. Brandt, N. Lopez-Salas, F. Lai, Q. Li, T. Liu, R. Amal, X. Lu, M. Antonietti, *Angew. Chem. Int. Ed.*, 134, e202206915 (2022).
- (4) Z. Lin, Q. Zhang, J. Pan, C. Tsounis, A. A. Esmailpour, S. Xi, H. Y. Yang, Z. Han, J. Yun, R. Amal, X. Lu, Atomic Co decorated free-standing graphene electrode assembly for efficient hydrogen peroxide production in acid, *Energy Environ. Sci.*, 15, 1172-1182 (2022).
- (5) Q. Zhang, Z. L. Z. Ru, R. Daiyan, P. Kumar, J. Pan, X. Lu, R. Amal, Surface Reconstruction Enabled Efficient Hydrogen Generation on a Cobalt–Iron Phosphate Electrocatalyst in Neutral Water, *ACS Appl. Mater. Interfaces*, 13, 45, 53798–53809 (2021).
- (6) Q. Zhang, P. Kumar, X. Zhu, R. Daiyan, N. M. Bedford, K. Wu, Z. Han, T. Zhang, R. Amal, X. Lu, Electronically modified atomic sites within a multicomponent Co/Cu composite for efficient oxygen electroreduction, *Adv. Energy Mater.*, 11, 2100303 (2021).
- (7) Y. Zhao, W. Jiang, J. Zhang, E. C. Lovell, R. Amal, Z. Han, X. Lu, Anchoring Sites Engineering in Single-Atom Catalysts for Highly Efficient Electrochemical Energy Conversion Reactions, *Adv. Mater.*, 33, 2102801 (2021).

- (8) Q. Zhang, X. Tan, N. M. Bedford, Z. Han, L. Thomsen, S. Smith, R. Amal, X. Lu, Direct insights into the role of epoxy groups on cobalt sites for acidic H<sub>2</sub>O<sub>2</sub> production, *Nat. Commun.*, 11, 4181 (2020).
- (9) X. Wong, Y. Zhuo, Y. Shen, Numerical analysis of hydrogen bubble behaviour in a zero-gap alkaline water electrolyser flow channel, *Ind. Eng. Chem. Res.*, 60, 33, 12429-12446 (2021).

## 6. Conclusion and Future Plans

### 6.1 Conclusion

A stand-alone, scalable prototype PVE system, that is able to generate green hydrogen from sunlight through photovoltaic electricity powered water electrolysis, with a high STH efficiency is established. Through a smart management of both thermal and electrical energy produced from the CPV modules, the prototype PVE system can utilise the solar energy more efficiently than the conventional renewable water electrolysis devices. The high-performance PVE system comprises three principal integrated components: (i) a CPV module that generates electricity with a high STE efficiency; (ii) an alkaline water electrolyser cell employing high-performance cost-effective materials; and (iii) a heat exchanger system that can control the temperature of water electrolysis by either external heating source or waste heat from CPV device. Without CO<sub>2</sub> emission, the system is capable of producing hydrogen from solar energy more efficiently than the commercial water electrolysis technologies. In terms of development and performance, the PVE prototype:

- (i) can achieve a high solar-to-electricity conversion efficiency than the commercial Si-based PV technologies;
- (ii) enables a more efficient utilisation of solar energy by recycling the waste heat produced from CPV module into the water electrolysis system;
- (iii) can reach a much higher H<sub>2</sub> production efficiency during the water electrolysis compared with conventional alkaline water electrolysis technology in industry;
- (iv) demonstrates the practical feasibility of scaling up the PVE prototype into commercially available systems in industry (1 kW), which is in close collaboration with RayGen.
- (v) Progressed from TRL3 to TRL4;

Furthermore, computational modelling tools have been developed regarding the influence of flow channels on the water electrolysis performance. The two-phase flow behaviour in different flow channel designs is simulated. Based on the CFD simulation results, a novel and optimised flow channel design is proposed to lower the pressure drop of the electrolyser while maintaining the bubble removal efficiency. The in-depth analysis is expected to contribute to the flow channel design optimisation and electrolyser's performance improvement.



Outcomes from the Activity validates the feasibility of the proposed PVE system in generating renewable H<sub>2</sub> with a high efficiency and low cost. It provides a promising approach to convert/store the solar energy more efficiently, giving further insight into the management of renewable power resources. The technology highlights the importance of proper energy management, including heat and electricity, in achieving high-performance renewable hydrogen production in large scale. Experimental practices and techno-economic analysis both have shown the technology developed in the Activity is scalable, which suggests a low-cost green H<sub>2</sub> production approach with commercial perspectives.

## 6.2 Future Plans

The following activities have recently been progressed to further push forward the development of integrated PVE technology as well as transferring the knowledge into other applications:

- (i) Further grants applications for the adoption of the technology in large-scale setups (up to MW) to accelerate the widespread application of PVE technology for the production of green hydrogen;
- (ii) Projects relating to the application of PVE setups in other electrocatalysis processes for value-added green chemicals, such as hydrogen peroxide production via oxygen reduction reaction, methanol production by CO<sub>2</sub> reduction reaction, have commenced.

## Reference

- [1] Tembhurne S, Nandjou F, Haussener S. A thermally synergistic photo-electrochemical hydrogen generator operating under concentrated solar irradiation. *Nat Energy* 2019;4:399–407. <https://doi.org/10.1038/s41560-019-0373-7>.
- [2] Kong G, Mirsandi H, Buist KA, Peters EAJF, Baltussen MW, Kuipers JAM. Oscillation dynamics of a bubble rising in viscous liquid. *Exp Fluids* 2019;60:1–13. <https://doi.org/10.1007/s00348-019-2779-1>.
- [3] Majasan JO, Cho JIS, Dedigama I, Tsaoulidis D, Shearing P, Brett DJL. Two-phase flow behaviour and performance of polymer electrolyte membrane electrolyzers: Electrochemical and optical characterisation. *Int J Hydrogen Energy* 2018;43:15659–72. <https://doi.org/10.1016/j.ijhydene.2018.07.003>.
- [4] Aurecon, AEMO. 2020 Costs and Technical Parameter Review. 2020.
- [5] Graham C, Hayward P, Foster J, Havas L. GenCost 2021-22. 2022.
- [6] Böhm H, Zauner A, Rosenfeld DC, Tichler R. Projecting cost development for future large-scale power-to-gas implementations by scaling effects. *Appl Energy* 2020;264:114780. <https://doi.org/10.1016/j.apenergy.2020.114780>.

- [7] IRENA. Renewable Power Generation Costs in 2021. Abu Dhabi: 2022.
- [8] AEMO. AEMO costs and technical parameter review Report Final Rev 4 9110715. 2018.